A New Control Method for Smoothing PMSG-Based Offshore Wind Farm Output Power

Navid Ghardash khani *

Department of Electrical Engineering, Bandar Anzali Branch, Islamic Azad University, Bandar Anzali, Iran,Email: navid_gh@aut.ac.ir

Abstract

Nowadays, propagation of wind turbines makes challenges to supply safe power to the grid. Because of wind speed changes, supervisors are concerned to wind turbines, be able to produce appropriate electric power during the wind speed changes. As a matter of fact, investors are mostly like to invest on offshore wind farms, because of their more stable and continuous wind speed rather than onshore ones. Although offshore wind farms are more reliable than onshore ones, their power control is a very important issue. In this paper a method is presented to control wind farms output power. This method is able to fix wind farm output power even during the wind speed changes. On the other hand by this method, the wind farm is able to operate such as a PV BUS. The proposed wind farm configuration and control system is validated by simulation on MATLAB/Simulink software. We also formulate and model the wind turbine, VSC converters of HVDC link and the PMSG generator. Moreover they are modeled and simulated on d-q frame by MATLAB/Simulink.

Keywords: WECS (Wind Energy Conversion System), PMSG (Permanent Magnet Synchronous Generator), MPPT (Maximum Power Point Tracking), VSC (Voltage Source Converter),CSI(Current Source Inverter).
Article history: Received 11- JUL-2017; Revised 24-JUL-2017; Accepted 11-SEP-2017.

1. Introduction

Nowadays lots of wind turbines are using around the world because of their compatibility with the environment. It is expected that the wind turbines usage will propagate on the near future. This will cause important considerations in technical issues in wind farms connection to the grid [1]. WECSs are based on several technologies, such as DFIGs and PMSGs. Today, the PMSG-based WECS usage has spread out because of their significant advantages such as no need of excitation, low volume and weight and high precision [2]-[5].In [6], authors have proposed a configuration and control method, based on rectifying each turbine power by a diode rectifier and using a DC-DC converter right after each wind turbine. By series connection of wind turbines, and controlling the duty cycle of DC-DC converter, power control of the wind farm is being achievable. Also this method has some advantages such as no need of transformer and the ability of maximum power point tracking (MPPT). Although this method has many advantages, it has some disadvantages such as low reliability. Moreover, outage of each wind turbine can cause variations on HVDC link and decreasing of wind farm output power, instantaneously. In [7], a new configuration is proposed based on series and parallel connection of wind turbines, using CSIs. This configuration is suitable for numerous wind turbines connection. In this method, wind farms power control is not accurately. Moreover wind turbines outage may cause interrupts in power production. Similarly in reference [8], authors have proposed a configuration use parallel and series connection of wind turbines. This configuration benefits VSCs connection with HVDC link. The proposed system has the advantages and disadvantages of system proposed in reference [7]. In references [9] and [10] authors have suggested using energy storage systems (EES) such as SMES (Super conducive Magnetic Energy storage System) and flywheel to mitigate fluctuations of power produced by the wind turbine. Although their simulation results illustrate these systems can smooth wind power variations, the amount of energy stored in

EESs is limited and is not suitable for large changes in wind speed. In reference [11] authors benefit wind speed prediction for power smoothing of wind turbines. Although this method is mostly useful for power smoothing, there is not appropriate control on extracted power from the wind farm in this method. There are different topologies and control systems for wind farms connected to the grid via HVDC link [12]-[13]. In reference [12], different MTDC (Multi Terminal DC) connections of wind turbines with their advantages and disadvantages have been analyzed. In reference [13], wind turbines connected to the grid by CSIs, based on series parallel and their different combinations have been analyzed.

The aim of this paper is to propose a new configuration of offshore wind turbines using HVDC-light link to control and fix wind farm output power during wind speed changes.

The organization of this paper is as follows: On the next section, the model of the wind conversion energy system (WECS), based on PMSG, is presented. Furthermore, modeling and control of PMSG using vector control is analyzed on this section. On the third section, a configuration of the offshore wind farm, connected to the onshore grid by HVDC cable is presented. Also its control method is proposed and analyzed. Fourth section discusses the simulation results of the proposed system by MATLAB/Simulink and finally the paper's main results are summarized on the conclusion section.

2. Wind Energy Conversion System

The wind energy conversion system (WECS), used in this paper includes the wind turbine, PMSG, HVDC-light link, its VSC converters and transformers. In this system, the wind energy is extracted by wind turbine and transmitted to a three phase PMSG by a constant ratio gear box which converts the mechanical power into electrical one and finally transmitted by a HVDC-light link, connected to the grid. Table1 illustrates the parameters of wind turbine and generator.

Table.1.
Parameters of wind turbine and generator

Parameter and dimension	*Symbol*	*Value*
Air density (kg/m^3)	ρ	1.28
Blade length (m)	R	30
Wind speed (m/s)	V_w	Variable
Power coefficient	C_p	Variable
Turbine angular speed (Rad/s)	ω	Variable
Turbine Tip speed ratio	Λ	Variable
Pitch angle of wind turbine (deg)	β	0
Stator resistance (Ohm)	R_s	0.01
Direct & quadrature stator inductance (mH)	L_d,L_q	0.165
Inductance of stator (mH)	L_s	0.165
Stator linkage flux (Volt.second)	λ	2.5
Pair poles number	P	2
Inertia of turbine and PMSG ($kg.m^2$)	J	2.86×10^5
Gearbox ratio	N_{Gear}	45

A) Wind turbine modeling

The turbine wind power ($P_{Extracted}$) and mechanical torque (T_m) modeling are described by (1)-(3), [4-15].

$$P_{Extracted} = \frac{1}{2}.C_p(\lambda,\beta)\rho A V_w^3 \quad (1)$$

$$\lambda = \frac{w_t R}{V_w} \quad (1)$$

$$T_m = \frac{P_{Extracted}}{w_t} \quad (2)$$

where, $C_p(\lambda,\beta)$ is the aerodynamic efficiency of the wind turbine, which is depended on the tip speed ratio and pitch angle of the wind turbine. This efficiency is related to λ and β by following equations. Although pitch angle control system is a conventional method in wind turbine systems, it has low dynamic response and is not sufficient enough to cooperate in fast output power of wind turbines changes [16]. As a matter of fact, in the proposed method, β is suggested to maintain constant and is operated at zero [17].

Figure 1 illustrates the $C_p(\lambda,\beta)$ curve for three types of pitch angels.

$$C_p(\lambda,\beta) = C_1(C_2\frac{1}{\Lambda} - C_3\beta - C_4\beta^{C5} - C_6)e^{-\frac{C_7}{\Lambda}} \quad (3)$$

where, Λ is given by (5).

$$\frac{1}{\Lambda} = \frac{1}{\lambda + C_8\beta} - \frac{C_9}{1+\beta^3} \quad (4)$$

The coefficients $c_1 - c_9$ are different for wind turbines and are selected as listed table 2 [15].

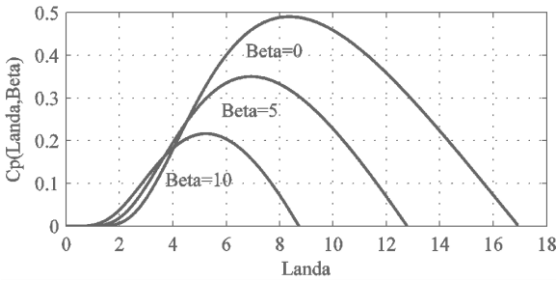

Fig. 1. $C_p(\lambda,\beta)$ Curve.

Table.2.
Wind turbine coefficients and parameters

Coefficient	C_1	C_2	C_3	C_4
Value	0.44	125	0.4	0.022
Coefficient	C_5	C_6	C_7	C_8
Value	2	6.94	16.5	0.08

B) PMSG d-q modeling

Permanent magnet synchronous generator (PMSG) is one of the conventional generators used in wind turbine systems. In the follows, modeling of this type of generator in *d-q* frame is proposed [17-18]. By using figure 2, the direct and quadrature voltage of the stator can be written as (6).

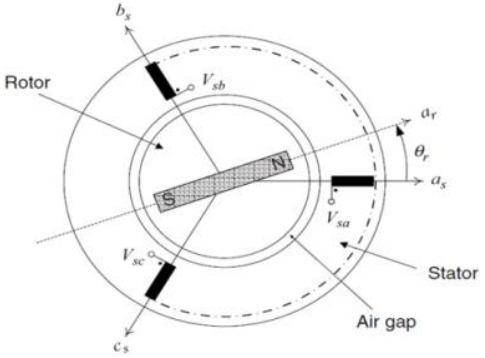

Fig. 2. PMSG schematic

$$\begin{bmatrix} v_d \\ v_q \end{bmatrix} = \begin{bmatrix} L_d & 0 \\ 0 & L_q \end{bmatrix} \begin{bmatrix} \frac{di_d}{dt} \\ \frac{di_q}{dt} \end{bmatrix} + \begin{bmatrix} R_s & 0 \\ 0 & R_s \end{bmatrix} \begin{bmatrix} i_d \\ i_q \end{bmatrix} + \begin{bmatrix} -L_q pw_r i_q \\ L_d pw_r i_d + \lambda pw_r \end{bmatrix} \quad (5)$$

where p is Laplace differential operator. In PMSG which is not a salient pole machine, we have,

$$L_d = L_q = L_s$$

So:

$$\frac{d\lambda_s}{dt} = v_s - R_s i_s \quad (6)$$

$$\frac{d(\vec{\lambda}_{dq} e^{j\omega_s t})}{dt} = \vec{v}_{dq} - R_s \vec{i}_{dq} e^{j\omega_s t} \quad (7)$$

$$\frac{d}{dt}\begin{bmatrix} \lambda_d \\ \lambda_q \end{bmatrix} = \begin{bmatrix} 0 & w_s \\ -w_s & 0 \end{bmatrix} \begin{bmatrix} \lambda_d \\ \lambda_q \end{bmatrix} + \begin{bmatrix} -R_s & 0 \\ 0 & -R \end{bmatrix} \begin{bmatrix} i_d \\ i_q \end{bmatrix} + \begin{bmatrix} v_{sd} \\ v_{sq} \end{bmatrix} \quad (8)$$

The electrical power of the machine can be determined by the following equations.

$$P = \frac{3}{2}\begin{bmatrix} i_d \\ i_q \end{bmatrix}^T \begin{bmatrix} v_{sd} \\ v_{sq} \end{bmatrix} = \frac{3}{2}\begin{bmatrix} i_d \\ i_q \end{bmatrix}^T \left\{ \frac{d}{dt}\begin{bmatrix} \lambda_d \\ \lambda_q \end{bmatrix} - \begin{bmatrix} 0 & w_s \\ -w_s & 0 \end{bmatrix} \begin{bmatrix} \lambda_d \\ \lambda_q \end{bmatrix} - \begin{bmatrix} -R_s & 0 \\ 0 & -R \end{bmatrix} \begin{bmatrix} i_d \\ i_q \end{bmatrix} \right\} \quad (9)$$

$$P = \frac{3}{2} R_s (i_d^2 + i_q^2) + \frac{3}{2}(i_d \frac{d\lambda_d}{dt} + i_q \frac{d\lambda_q}{dt}) + w_s \frac{3}{2}(\lambda_d i_q - \lambda_q i_d) \quad (10)$$

The electromagnetic torque can be deduced by (11).

$$T_e = \frac{P}{w_r} = \frac{3}{2} p(\lambda_d i_q - \lambda_q i_d) \quad (11)$$

$$T_e = \frac{3}{2} p[\lambda_m i_q + (L_d - L_q) i_d i_q] \quad (12)$$

$$T_e = \frac{3}{2} p[\lambda i_q] \quad (13)$$

C) VSC average model and its control

In this section, the modeling of the VSC is presented. It is connected to PMSG in order to control the torque, power and rotational speed. Figure 3 illustrates the circuit of this system [18-19].

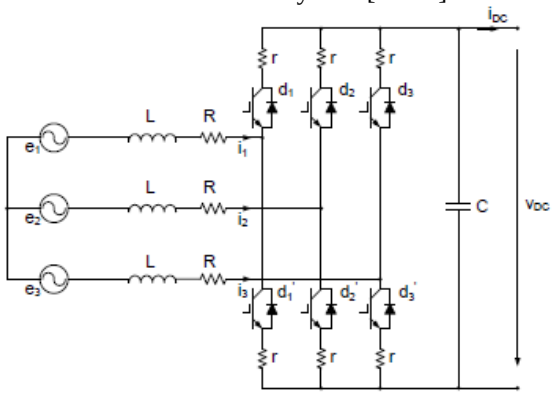

Fig. 3. Model of the VSC.

In Figure 3, we have:

$$\begin{aligned} L\frac{di_a}{dt} + Ri_a &= V_{ta} - U_a \\ L\frac{di_b}{dt} + Ri_b &= V_{tb} - U_b \\ L\frac{di_c}{dt} + Ri_c &= V_{tc} - U_c \end{aligned} \quad (14)$$

where, V_{ta}, V_{tb}, V_{tc} are output voltages of VSC. By using Fourier's series of these periodical voltages, the (15) can be rewritten as follows.

$$\begin{aligned} L\frac{di_a}{dt} + Ri_a &= (-U_a + \frac{1}{T_s}\int_{t-T_s}^{T_s} V_{ta}(\tau)d\tau) + \sum_{h=1}^{\infty}[a_{ah}\cos(hw_s\tau) + b_{ah}\sin(hw_s\tau)] \\ L\frac{di_b}{dt} + Ri_b &= (-U_b + \frac{1}{T_s}\int_{t-T_s}^{T_s} V_{tb}(\tau)d\tau) + \sum_{h=1}^{\infty}[a_{bh}\cos(hw_s\tau) + b_{bh}\sin(hw_s\tau)] \\ L\frac{di_c}{dt} + Ri_c &= (-U_c + \frac{1}{T_s}\int_{t-T_s}^{T_s} V_{tc}(\tau)d\tau) + \sum_{h=1}^{\infty}[a_{ch}\cos(hw_s\tau) + b_{ch}\sin(hw_s\tau)] \end{aligned} \quad (15)$$

where, we have:

$$\begin{aligned} a_{ih} &= \frac{2}{T_s}\int_{t-T_s}^{T_s} (V_{ti}(\tau)\cos(hw_s\tau)d\tau) \\ b_{ih} &= \frac{2}{T_s}\int_{t-T_s}^{T_s} (V_{ti}(\tau)\sin(hw_s\tau)d\tau) \end{aligned} \quad (16)$$

Equation (16) is a set of differential equations which has one AC and one DC response. Although by using the superposition law, these two components can be separately analyzed, the AC component is negligible if the switching frequency is too larger than R/L. Therefore, (16) can be rewritten as follows:

$$L\frac{di_a}{dt}+Ri_a=(-U_a+\frac{1}{T_s}\int_{t-T_s}^{T_s}V_{ta}(\tau)d\tau)$$
$$L\frac{di_b}{dt}+Ri_b=(-U_b+\frac{1}{T_s}\int_{t-T_s}^{T_s}V_{tb}(\tau)d\tau) \quad (17)$$
$$L\frac{di_c}{dt}+Ri_c=(-U_c+\frac{1}{T_s}\int_{t-T_s}^{T_s}V_{tc}(\tau)d\tau)$$

For a sinusoidal PWM, (18) can be rewritten as bellow:

$$L\frac{di_a}{dt}+Ri_a=(-U_a+m_a\frac{V_{dc}}{2})$$
$$L\frac{di_b}{dt}+Ri_b=(-U_b+m_b\frac{V_{dc}}{2}) \quad (18)$$
$$L\frac{di_c}{dt}+Ri_c=(-U_c+m_c\frac{V_{dc}}{2})$$

These equations can be illustrated as Figure 4.

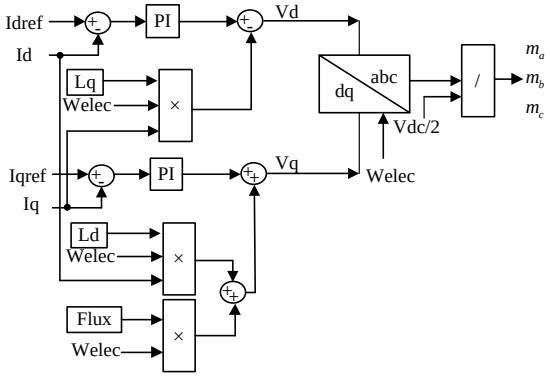

Fig. 4. Control Block diagram of VSC.

3. Proposed configuration of wind turbines and their control system

As discussed on the introduction, there are different configurations on the wind turbines connection in wind farms. Although these configurations have appropriate advantages, they are not suitable enough to control the output power of the wind farm accurately. To overcome this problem, following configuration is proposed to control and fix wind farm output power even during wind speed variations. The wind farm turbines are connected to the grid through a HVDC link as shown in figure 5. In this configuration, $n-j$ number of wind turbines and their VSCs operate at MPPT mode and j number turbines operate at power control mode. The power control mode makes the ability of fine tuning for these turbines. As shown in the following equations, the MPPT and power control operation modes are achievable by controlling $i_{q_{ref}}$.

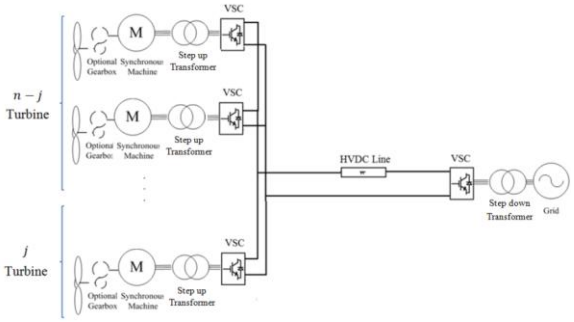

Fig. 5. Proposed configuration of wind turbines connection

A) MPPT and power control algorithm

In this part, we are concerned to control wind turbine rotational speed to track λ_{opt}which obtains maximum power efficiency of wind turbine (Figure 1). Controlling the speed and torque of the machine makes the ability of output power control and MPPT algorithm being achievable. This feature is achievable by controlling $i_{q_{ref}}$operated to VSCs as discussed in the bellow. Following equations analyze this operation condition.

$$\lambda_{opt}=\frac{R\omega_{tur}}{V_w} \quad (19)$$

$$V_w=\frac{R\omega_{tur}}{\lambda_{opt}} \quad (20)$$

$$P_{opt}=\left(\frac{0.5\rho AR^3C_{p,\max}}{\lambda_{opt}^3}\right)w_{tur}^3 \quad (21)$$

By dividing output power to the rotational speed, electromagnetic torque is achievable [17].

$$T_{opt}=\left(\frac{0.5\rho AR^3C_{p,\max}}{\lambda_{opt}^3}\right)w_{tur}^2 \quad (22)$$

$$P_{opt}=Kw_{tur}^3 \quad (23)$$

$$T_{opt}=Kw_{tur}^2 \quad (24)$$

$$K_{opt}=\left(\frac{0.5\rho AR^3C_{p,\max}}{\lambda_{opt}^3}\right) \quad (25)$$

By using (14) and the above equations, $i_{q_{ref}}$ can be calculate as bellow.

$$i_{q_{ref}}=-\frac{1}{N_{Gear}\frac{3}{2}p\lambda_m}T \quad (26)$$

$$i_{q,ref}=-\frac{1}{N_{Gear}}\frac{T_{opt}}{\frac{3}{2}p\lambda_m}=-\frac{1}{N_{Gear}}\frac{\frac{1}{2}\rho A(\frac{R^3}{\lambda^3{}_{opt}})C_{p,\max}.w^2}{\frac{3}{2}p\lambda_m} \quad (27)$$

$i_{q_{ref}}$is applied to each VSC to control wind turbines operate at maximum power point. While the

purpose of control is power control of a wind turbine, $i_{q_{ref}}$ should be operated as bellow:

$$i_{q_{ref}=-\frac{1}{N_{Gear}}\frac{P_{applied}}{\frac{3}{2}P\lambda_m\omega}} \quad (28)$$

As discussed before, to produce constant output power of wind farm, we have to set $P_{power\ control}$ as bellow:

$$P_{Desierd} = (n-j).P_{MPPT} + P_{power\ control} \quad (29)$$

$$P_{power\ control} = j.P_{applied} \quad (30)$$

$$P_{MPPT}(V) = \frac{1}{2}\rho AV^3 c_{p_{opt}} \quad (31)$$

$$P_{applied}(V) = \frac{P_{Desired}-(n-j)P_{MPPT}(V)}{j}, \quad P_{applied} \le P_{MPPT} \quad (32)$$

If, $P_{applied} > P_{MPPT}$, j should be increased.

As wind speed (V) can be varied, consequently $P_{applied}(V)$ is variable. By combining (29) and (33), $i_{q_{ref}}$ which should be applied to VSC, is calculated as follows.

$$i_{q_{ref}=-\frac{1}{N_{Gear}}\frac{P_{Desired}-(n-j)P_{MPPT}(V)}{\frac{3}{2}P\lambda_m\omega j}} \quad (33)$$

4. Simulation Results

In this section, simulation is applied on 100 wind turbines. The simulation results are illustrated and analyzed as bellow. In the simulations the value of j and N are assumed to 20 and 100, respectively. Moreover, the $P_{Desired}$ is set to 220 MW.

Figures 6 and 7 illustrate the wind speed and $P_{applied}$ of power control turbines, respectively. Figure 8 shows the output power of turbines, operating at $MPPT$ mode.

Figure 9 illustrates the efficiency of wind turbines, operate in MPPT mode. The power efficiency is fixed to its maximum value by this algorithm. Also figure 10 illustrates the efficiency of power control wind turbines.

Figures 11 and 12 illustrate I_d and $I_{d_{reff}}$ of MPPT and power control wind turbines, respectively. Figure 13 and 14 illustrate I_q and $I_{q_{ref}}$ of MPPT and power control turbine, respectively.

Figure 15 shows the output power of wind farm, using the proposed method. Although the variation of wind speed is such as a noise, the total output power of wind farm is reinstated by the proposed algorithm. On the MPPT mode, all of the wind turbines operate at the maximum power point and the power control wind turbines controls the wind farm output power.

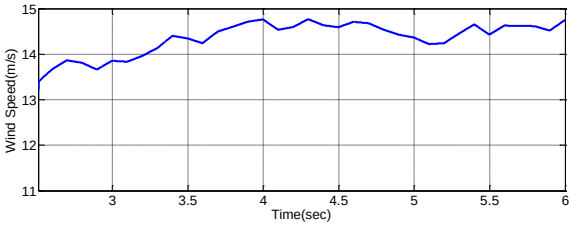

Fig. 6. Wind speed variations.

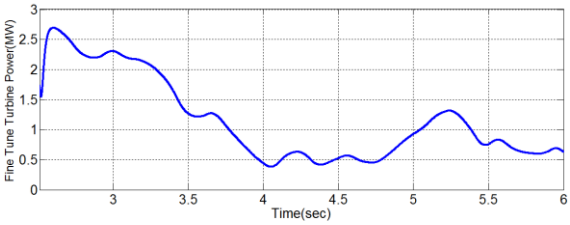

Fig. 7. $P_{applied}$ of power control turbines

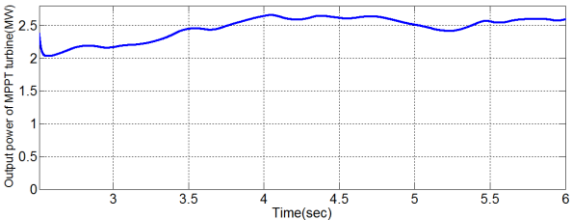

Fig. 8. P_{MPPT} of each of (n − j) turbines.

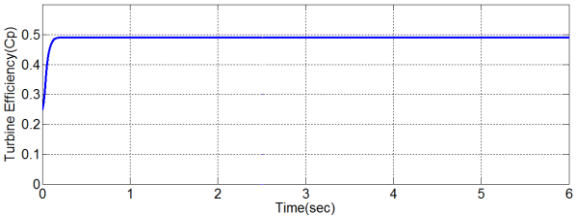

Fig. 9. Power coefficient of MPPT turbines.

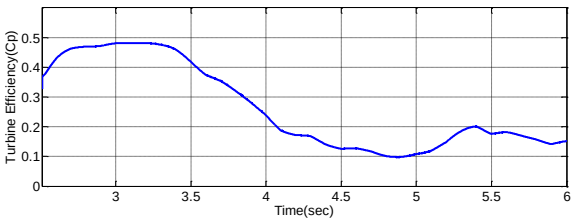

Fig. 10. Power coefficient of Float power turbines.

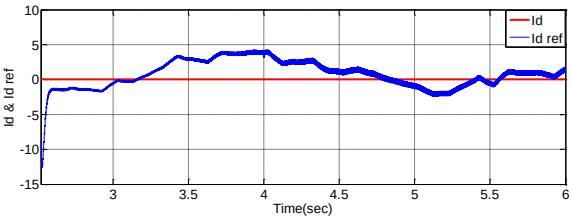

Fig. 11. I_d and $I_{d_{ref}}$ of MPPT turbine.

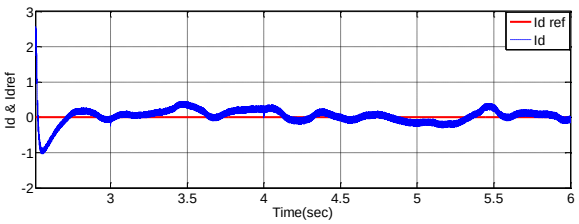

Fig. 12. I_d and $I_{d_{ref}}$ of power control turbine.

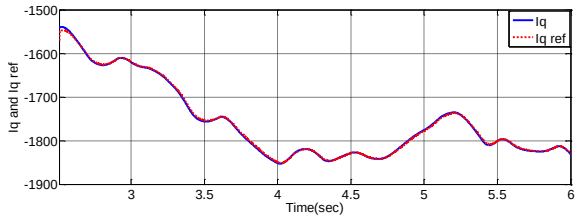

Fig. 13. I_q and $I_{q_{ref}}$ of MPPT turbine.

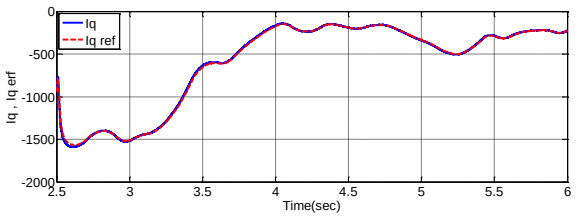

Fig. 14. I_q and $I_{q_{ref}}$ of power control turbine.

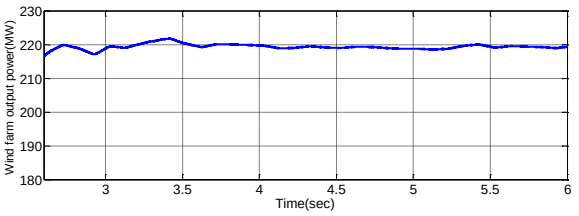

Fig. 15. Output power of wind farm.

5. Conclusion

In this paper, a new configuration of the offshore wind turbine connection to the onshore grid is proposed. The proposed system is able to reinstate wind farm output power due to wind speed variations. This system, benefits mitigating wind farm output power fluctuations. Considering the wind speed and output power, the number of turbines in power control mode (j), and the turbines in MPPT mode $(n-j)$ can be calculated. The proposed system is studied by MATLAB/ Simulink for a noise wind speed conditions. The simulation results validated the proposed control method operation.

References

[1] Chih-Ming Hong, Chiung-Hsing Chen, Chia-Sheng Tu, ”Maximum power point tracking-based control algorithm for PMSG wind generation system without mechanical sensors” ,Energy Conversion and Management,vol.69, 2013.

[2] Whei-Min Lin, Chih-Ming Hong, Ting-Chia Ou, Tai-Ming Chiu, “Hybrid intelligent control of PMSG wind generation system using pitch angle control with RBFN” ,Energy Conversion and Management ,vol.52 ,2011.

[3] I. S¸ erban, C. Marinescu, “Modeling of small wind turbines based on PMSG with diode bridge for sensorless maximum power tracking” Renewable Energy ,vol.43, 2012.

[4] Abdeldjalil Dahbi, Mabrouk Hachemi, Nasreddine Nait-Said, Mohamed-Said Nait-Sai, “Realization and control of a wind turbine connected to the grid by using PMSG” ,Energy Conversion and Management ,vol.84, 2012.

[5] Global wind and energy council, market forecast 2010-2014, available at: http://www.gwec.net/fileadmin/documents/Publications/GlobalWind2007report/market/forecast 2010-2014.JPG.

[6] M. Kesraoui, N. Korichi, A. Belkadi, “Maximum power point tracker of wind energy conversion system” Renewable Energy ,vol.36, 2011.

[7] Etienne Veilleux, Peter W. Lehn, “Interconnection of Direct-Drive Wind Turbines Using a Series-Connected DC Grid” IEEE Transactions on sustainable energy, vol. 5, 2014.

[8] Dragan Jovcic, “Offshore wind farm with a series multiterminal CSI HVDC” Electric Power Systems Research, 2007.

[9] Oriol Gomis-Bellmunt, Jun Liang, Janaka Ekanayake, Rosemary King, Nicholas Jenkins, “Topologies of Multi terminal HVDC-VSC transmission for large offshore wind farms” ,Electric Power Systems Research. 2010.

[10] Zhang Xinyu, Dong Lei, “A smooth scheme of wind power generation based on wind power prediction” International Conference on Transportation, Mechanical, and Electrical Engineering (TMEE) , 2011.

[11] Issarachai Ngamroo and Tanapon Karaipoom, “Cooperative Control of SFCL and SMES for Enhancing Fault Ride Through Capability and Smoothing Power Fluctuation of DFIG Wind Farm”, IEEE Transactions on applied superconductivity, vol. 24, no. 5, 2014.

[12] Takayuki Kawaguchi, Tsukasa Sakazaki, Takanori Isobe, and Ryuichi Shimada, “Offshore Wind-Farm Configuration Using Diode Rectifier with MERS in Current Link Topology” IEEE Transactions on Industrial Electronics, vol. 60, no. 7, 2013.

[13] V. Akhmatov” Analysis of dynamic behavior of electric power systems with large amount of wind power” PhD. Dissertation, Dept. Elect. Eng., Harvard Univ., 2003.

[14] A. M. Hemeida, W. A. Farag, and O. A. Mahgoub” Modeling and control of direct driven PMSG for ultra large wind turbines” World Academy of Science, Engineering and Technology vol. 59, 2011.

[15] Xibo Yuan, Yongdong Li, “Control of variable pitch and variable speed direct-drive wind turbines in weak grid systems .with active power balance” IET Renewable Power Generation, 2013.

[16] O. Gomis-Bellmunt, A. Junyent-Ferre´, A. Sumper, and J. Bergas-Jane, "Control of a Wind Farm Based on Synchronous Generators With a Central HVDC-VSC Converter," IEEE Transactions on Power Systems, vol. 26, 2011.

[17] V. Akhmatov, “Analysis of dynamic behavior of electric power systems with large amount of wind power,” PhD. Dissertation, Dept. Elect. Eng., Harvard Univ., 2003.

[18] A. M. Hemeida, W. A. Farag, and O. A. Mahgoub, "Modeling and control of direct driven PMSG for ultra large wind turbines," World Academy of Science, Engineering and Technology, vol. 59, 2011.

[19] I. Stan, "Control of VSC-based HVDC transmission system for offshore wind power plants," Master, Departament of Energy Tehnology, Aalborg University, Denmark, 2010.

[20] A. Yazdani and R. Iravani, “Voltage-sourced converters in power systems,” IEEE Wiley, 2010.